Electronic Supplementary Material (ESI) for Journal of Materials Chemistry C.

SUPPORTING INFORMATION

Anomalously persistent p-type behavior of WSe_2 field-effect transistors by oxidized edge-induced Fermi-level pinning

Tien Dat Ngo[1†], Min Sup Choi[1†], Myeongjin Lee[1], Fida Ali[1], and Won Jong Yoo[1*]

[1]SKKU Advanced Institute of Nano Technology, Sungkyunkwan University, Suwon, Gyeonggi-do 16419, Korea

[†] These authors contributed equally to this work.

[*] e-mail: yoowj@skku.edu

Keywords: 2D semiconductors, Fermi-level pinning, plasma etching, edge contacts, tungsten oxide

Stacking and fabrication process of the hBN/WSe_2/hBN heterostructure

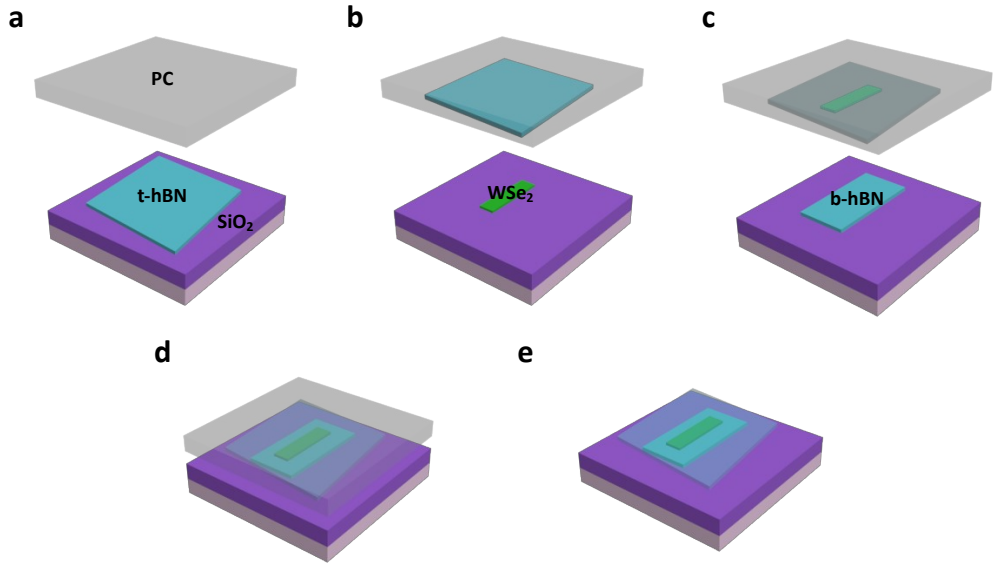

Figure S1. Consecutive pick-up of (a) top-hBN (t-hBN), (b) WSe_2, (c) bottom-hBN (b-hBN) by dry transfer using a PC polymer. (d) Transfer of hBN/WSe_2/hBN heterostructure onto SiO_2/Si substrate, followed by (e) rinse with chloroform to remove the PC.

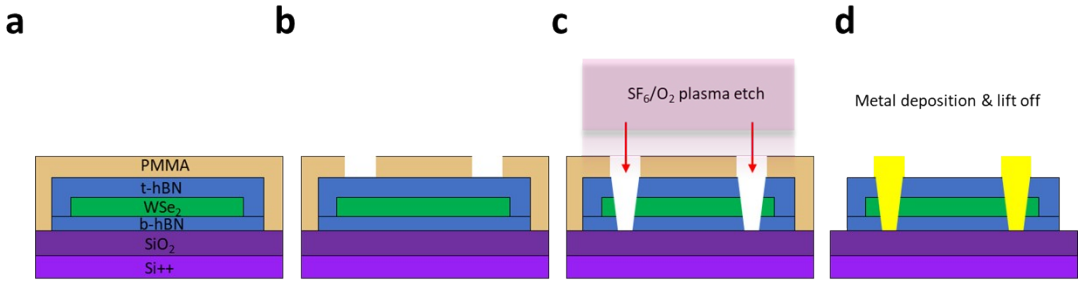

Figure S2. (a, b) Patterning of hBN/WSe_2/hBN heterostructure via electron beam lithography to form the edge contact regions. (c) SF_6/O_2 ICP etching to expose the edge of WSe_2. (d) Deposition of metals on the etched heterostructure via electron beam deposition.

Contact resistance extraction from Y-function method

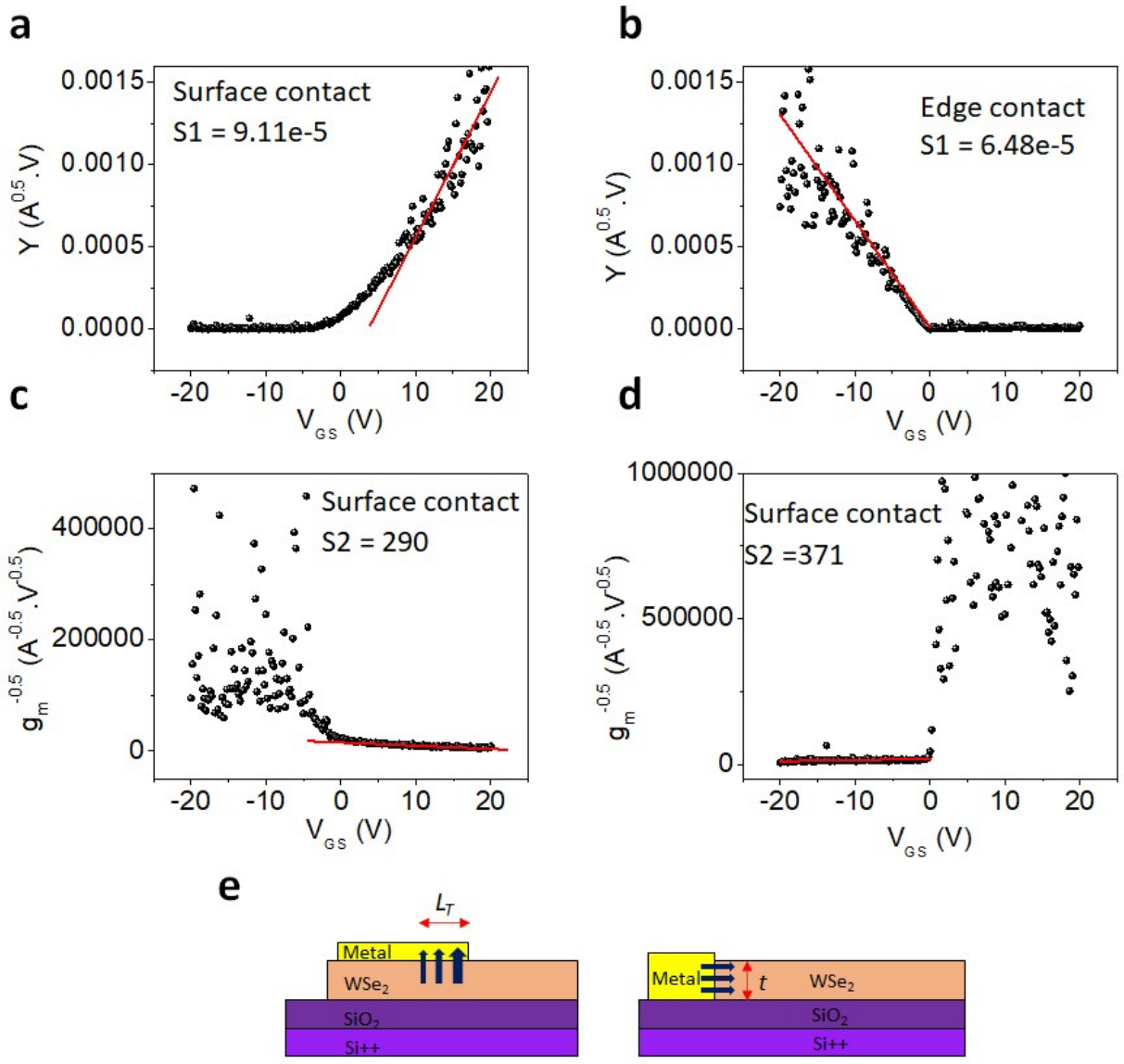

Figure S3. (a, b) The plots of $I_{DS}/\sqrt{g_m}$ and (c, d) $1/\sqrt{g_m}$ as a function of V_{GS} for WSe_2 FETs with Pd surface and In edge contacts, in which S1 and S2 represent the slopes of each curve. (e) Schematic of carrier transport at the surface and edge contacts.

Figure S3 shows the extraction of contact resistance from our devices by Y-function method.[1] With the Y-function method, the contact resistance can be extracted directly from the measured transfer curve. The Y-function is expressed by,

$$Y = \frac{I_{DS}}{\sqrt{g_m}}, \quad (1)$$

where I_{DS} is the drain current and $g_m = \frac{\partial I_{DS}}{\partial V_{GS}}$. From the slopes of Y vs. V_{GS} (S1) and $1/\sqrt{g_m}$ vs. V_{GS} (S2) as shown in Fig. S3 (a-d), we can extract the contact resistance by the following equation,

$$R_c = S_1^{-1} S_2 V_{DS}. \quad (2)$$

The contact resistance extracted from the equation (2) for surface and edge contacts are 3.2 MΩ and 5.7 MΩ, respectively. Since both contacts have different contact area according to the contact geometry, we normalize the contact resistance by the contact area to extract the contact resistivity for a fair comparison between surface and edge contacts, as depicted in **Figure S3**(e). For the surface contact, Moon *et al* stated that the transfer length (L_T) is ~ 0.23 μm for surface contacted WSe_2 device[2] thus the contact area is L_T multiplied by channel width (W = 3 μm in our device). In contrast, the contact area for edge contact is thickness of flake (t = 10 nm) multiplied by channel width (W = 13 μm). Thus, the contact resistivity of the devices calculated by the below equation,

$$\rho_c = R_c \cdot W \cdot t(L_t). \quad (3)$$

The calculated contact resistivities of surface and edge contacts are 2.2 MΩ·μm^2 and 0.741 MΩ·μm^2, respectively.

Table S1. Contact resistivity extracted from Y-function method for edge and surface contacts.

Contact methods	Edge			Surface	
Metals	Cr	Pd	In	Pd	In
S_1	6.6e-5	3.2e-5	6.5e-5	9.1e-5	1e-4
S_2	1074	1358	371	290	431
R_C (MΩ)	16	42	5.7	3.2	4.3
L_t (t) (μm)	1e-2	5e-3	1e-2	3.4e-1	2.3e-1
W (μm)	11	15	13	3	3
ρ_c (MΩ·μm^2)	1.8	3.2	0.74	3.25	3

Analysis on the metal-WSe_2 interface by EDS and electrical characterization

Figure S4 shows the EDS mapping results on STEM images at the metal-WSe_2 interface with two separate WSe_2 and metal regions as the white solid line indicates. The W and Se signals were clearly intensified within the WSe_2 region while the In signal was mostly detected in the metal region. As the EDS line profile in **Fig. 2**(d) showed the presence of oxygen atoms at the metal-WSe_2 interface clearly, the EDS mapping also confirmed the presence of the oxide layer as shown in **Fig. S4**(d) as the oxygen signals were accumulated at the metal-WSe_2 interface. We also observed the diffusion of In and Cr atoms into the oxide layer as shown in EDS line profiles near the oxide region of **Fig. S4**(f),(g). The formation of the oxide layer was attributed to the air exposure immediately after etching, as evidenced from the electrical characteristics of the edge contact WSe_2 devices after oxygen-free gas mixture etching and with monolayer channel, as shown in **Fig. S5**. A n-type behavior observed in $MoSe_2$ edge contacted device (**Fig. S6**) suggested that the formation of oxide layer is a unique feature of WSe_2.

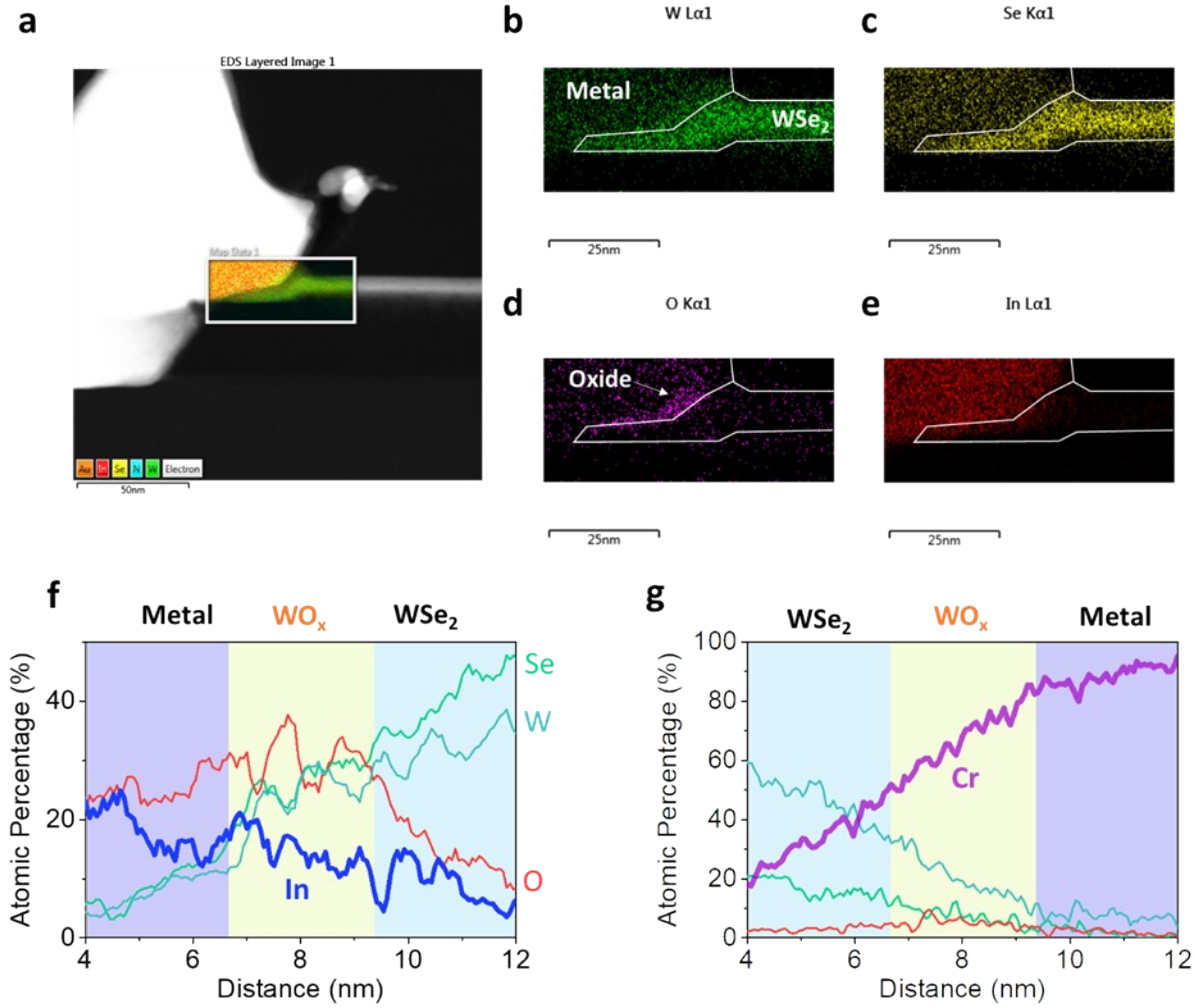

Figure S4. (a) EDS mapping on a cross-sectional STEM image at the metal-WSe_2 interface. EDS mapping for (b) W, (c) Se, (d) O, and (e) In elements, respectively. Line profile of EDS near the oxide region showing atomic percentages of W, Se, O, (f) In, and (g) Cr elements from two different devices, respectively.

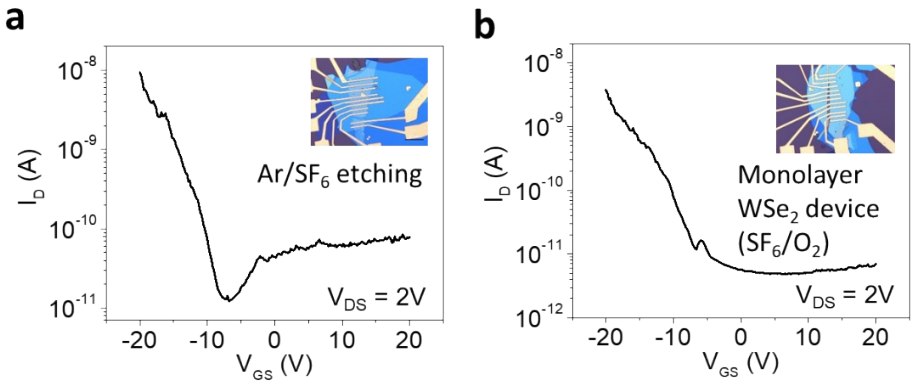

Figure S5. (a) Transfer curve of the WSe_2 edge contact device etched by using an oxygen-free Ar/SF_6 gas mixture. (b) Transfer curve of the monolayer WSe_2 edge contact device. The insets are optical micrographs of the devices.

Performances of the $MoSe_2$ edge contact device

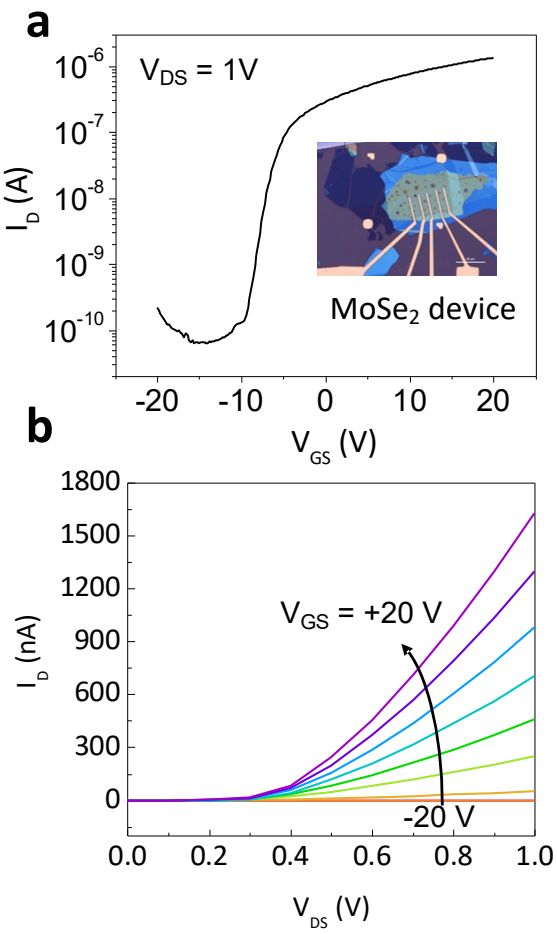

Figure S6. (a) Transfer and (b) output curves of the $MoSe_2$ edge contact device. The inset is optical micrograph of the device.

Performances of the WSe_2 edge contact device with various metals

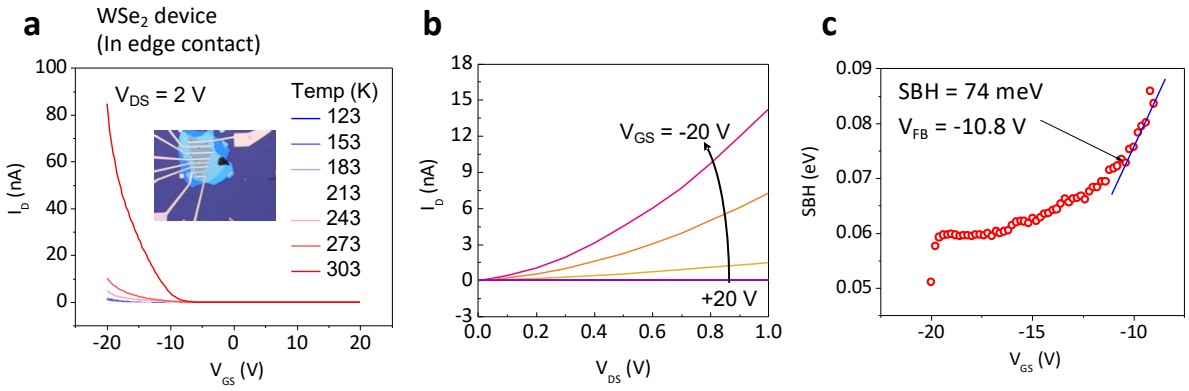

Figure S7. (a) Temperature dependent transfer curves, (b) output curves, and (c) SBH extraction at the flat band condition of the WSe_2 device with In edge contacts.

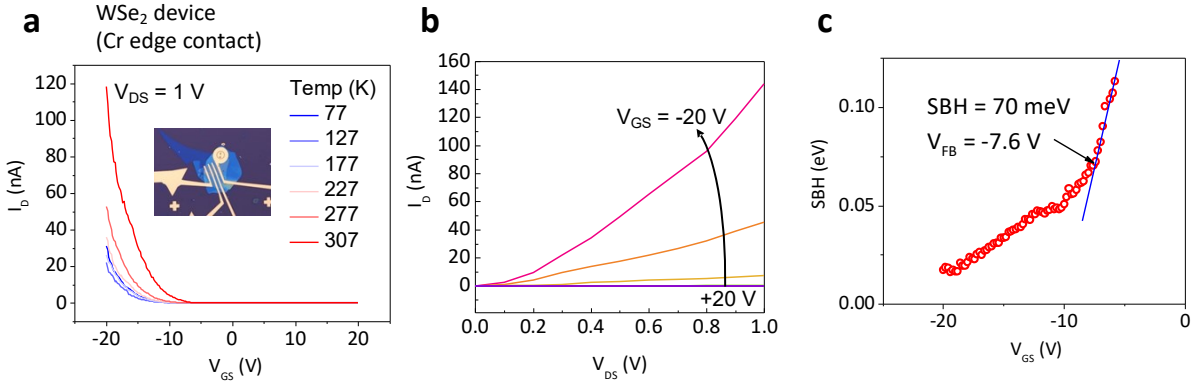

Figure S8. (a) Temperature dependent transfer curves, (b) output curves, and (c) SBH extraction at the flat band condition of the WSe_2 device with Cr edge contacts.

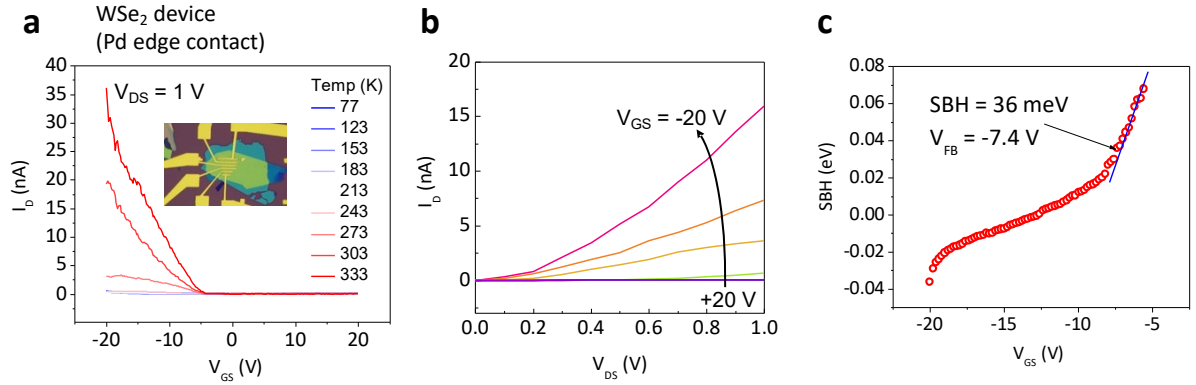

Figure S9. (a) Temperature dependent transfer curves, (b) output curves, and (c) SBH extraction at the flat band condition of the WSe_2 device with Pd edge contacts.

KOH treated and In edge contacted WSe_2 device

Figure S7-S9 demonstrated a strong Fermi-level pinning with nearly constant SBH obtained in the WSe_2 edge contact devices due to the presence of oxide layer. To remove the layer, we dipped the etched sample in a 1M KOH solution for 10 s, which typically eliminates the oxide layer within a few seconds, prior to metal deposition as illustrated in **Fig. S10**(a). The KOH treated WSe_2 FET with In edge contacts showed an n-type dominated behavior, as shown in **Fig. 4**(c) and **Fig. S10**(c) which was the same results typically observed from the In contacted WSe_2 devices. As the potassium ions can n-dope the 2D materials, we have also tested the effect of remained ions by comparing transfer curves before and after KOH treatment. As shown in **Fig. S11**, no noticeable change was observed, confirming that potassium ions have negligible doping effect in WSe_2 edge-contacted devices.

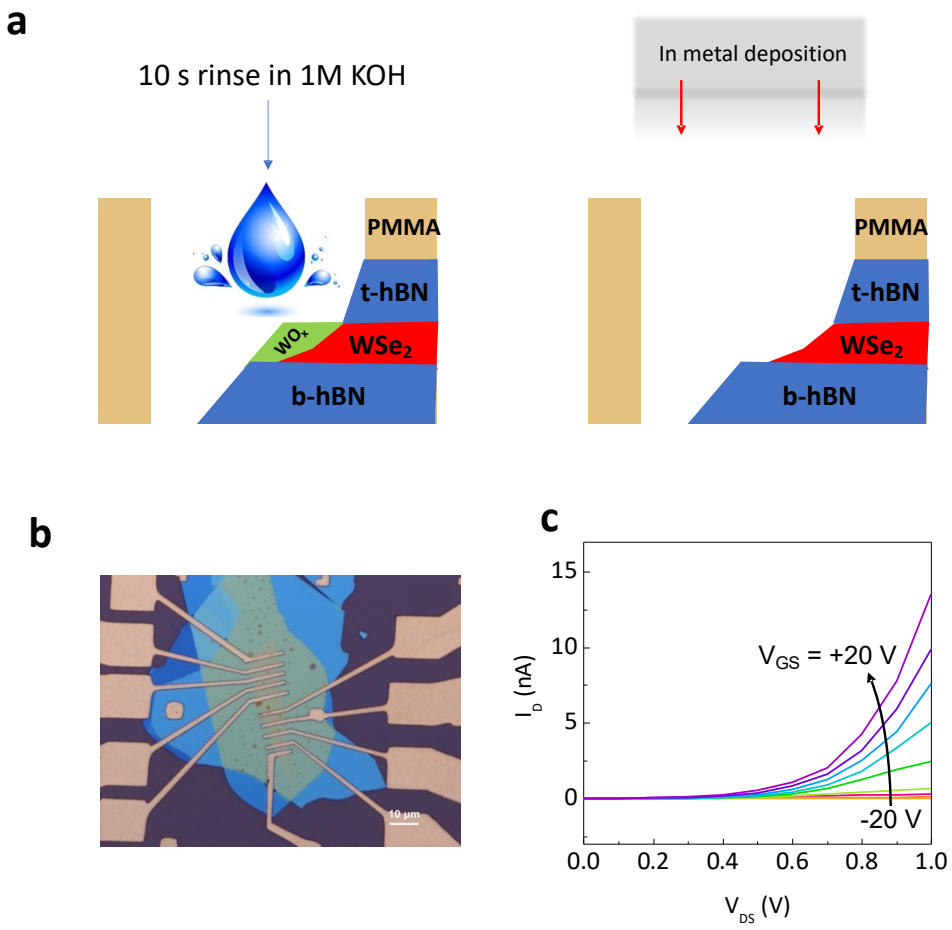

Figure S10. (a) Illustrations of KOH wet treatment and subsequent In metal deposition for a WSe_2 edge contact device. (b) Optical microscopic image and (c) output curves of the KOH treated WSe_2 edge contact device.

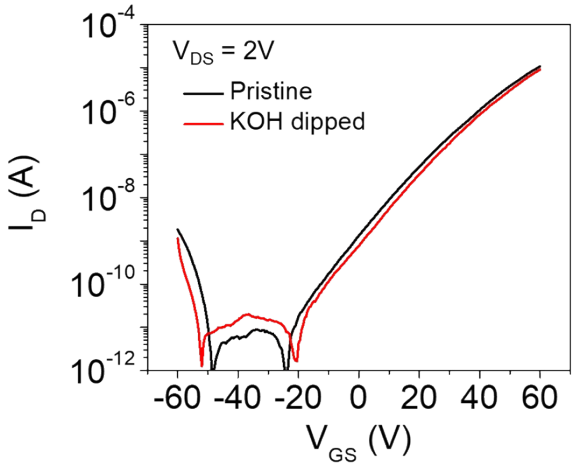

Figure S11. Transfer curves of WSe_2 device for pristine and after a 10-s KOH dip.

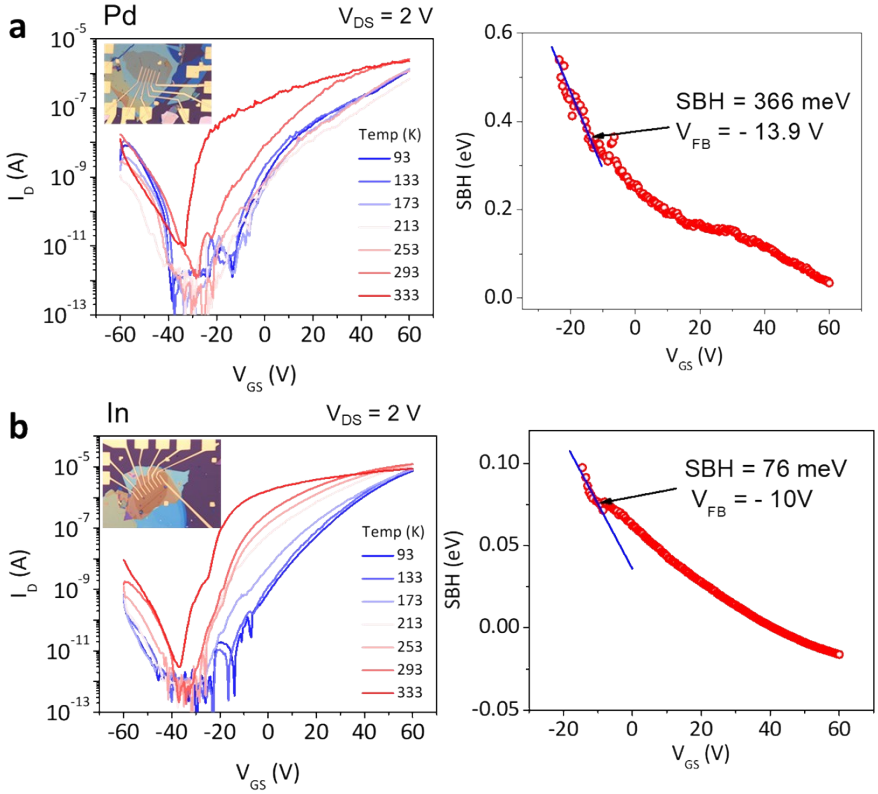

Figure S12. Temperature dependent (a) electrical characterization and (b) extracted SBH for Pd and In edge-contacted WSe_2 devices with KOH treatments to remove oxide layer.

References

1. C. Liu, Y. Xu, and Y.-Y. Noh, *Mater. Today,* 2015, **18**, 79-96.
2. I. Moon, M. S. Choi, S. Lee, A. Nipane, J. C. Hone and W. J. Yoo, *2D Mater.,* 2021, **8**, 045019.